

Anomaly in the tunneling $I(V)$ characteristics of $\text{Bi}_2\text{Sr}_2\text{CaCu}_2\text{O}_{8+x}$

A. Mourachkine

Free University of Brussels, B-1050 Brussels, Belgium

Submitted 12 May 2003

Tunneling measurements have been carried out on slightly overdoped $\text{Bi}_2\text{Sr}_2\text{CaCu}_2\text{O}_{8+x}$ single crystals below and above the critical temperature by break-junctions and in-plane point-contacts. An anomaly was found in the tunneling $I(V)$ characteristics. Analysis of the data shows that the anomaly is caused by the superconducting condensate. In the extracted $I(V)$ characteristics of the condensate, the constant asymptotics points to the presence of one-dimensionality in Bi2212. The anomaly found here puts additional constraints on the final theory of high- T_c superconductivity.

PACS: 74.25.-q, 74.50.+r, 74.72.Hs

Soon after the discovery of superconductivity (SC) in cuprates [1], it became clear that the concept of the Fermi liquid is not applicable to the cuprates: the normal state properties of cuprates are markedly different from those of conventional metals [2]. The pseudogap which manifests itself in electronic excitation spectra of cuprates above the critical temperature T_c , is one of the main features of high- T_c SCs. There is a consensus on doping dependence of the pseudogap in hole-doped cuprates: the magnitude of the pseudogap decreases as the hole concentration increases. Angle-resolved photoemission spectroscopy (ARPES) measurements performed in $\text{Bi}_2\text{Sr}_2\text{CaCu}_2\text{O}_{8+x}$ (Bi2212) show that the ARPES spectra consist of two *independent* contributions—from the pseudogap (hump) and the SC condensate (quasiparticle peak) [3]. As the temperature decreases, the quasiparticle peak appears in the spectra slightly above T_c on one side of the hump, meaning that the pseudogap and the SC gap coexist below T_c in Bi2212.

In addition to their peculiar normal-state properties, a number of experiments show that some SC properties of cuprates deviate from predictions of the BCS theory for conventional SCs [2]. For example, the BCS isotope effect is almost absent in optimally doped cuprates. As another example, let us compare tunneling data obtained in cuprates and theoretical predictions for conventional SCs. Figure 1 shows a theoretical $I(V)$ curve for classical SCs (Fig.6 in Ref. [4]) and a tunneling $I(V)$ characteristic obtained in an underdoped Bi2212 single crystal (Fig.1 in Ref.[5]). In the *tunneling* regime, depending on the normal resistance of a junction, the theoretical $I(V)$ curve at high positive (low negative) bias lies somewhat below (above) the normal-state curve, as shown in Fig.1a. In conventional SCs, the so-called Blonder-Tinkham-Klapwijk (BTK) predictions are verified by tunneling experiments. In cuprates, as one can

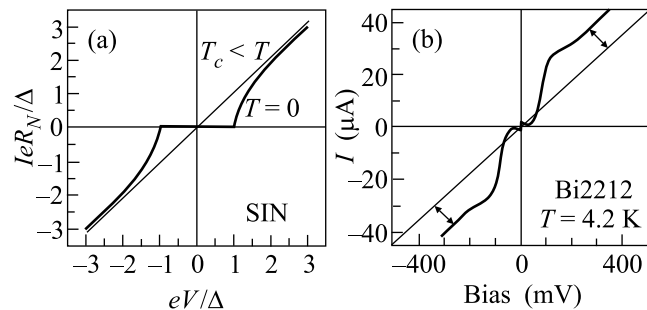


Fig.1. (a) Theoretical tunneling $I(V)$ characteristic at $T = 0$ for a SIN junction of a SC with the isotropic energy gap [4]. The line is the normal-state curve. (b) Measured $I(V)$ curve in a SIS junction of an underdoped Bi2212 single crystal with $T_c = 83$ K, obtained at $T = 4.2$ K [5]. The line is parallel to the $I(V)$ curve at high bias, and the arrows show the offset from the line

see in Fig.1b, the BTK theory is violated: the $I(V)$ curve at high positive (low negative) bias passes not below (above) the line which is parallel to the $I(V)$ curve at high bias but far above (below) the line. This anomaly cannot be explained by the d-wave symmetry of the order parameter. This question, for the first time, was raised elsewhere [6]. This finding is the main motivation of the present work.

The data shown in Fig.1b are obtained in an underdoped Bi2212 single crystal in a SC-insulator-SC (SIS) tunneling junction. If the anomaly is an intrinsic feature of SC in Bi2212, it has to be present in tunneling spectra in the overdoped region of Bi2212 as well. Second, if it is not a SIS-junction effect, it must also manifest itself in SC-insulator-normal metal (SIN) junctions. Third, the line in Fig.1b is not the normal-state curve, therefore it is necessary to obtain tunneling spectra in the normal state. Finally, knowing the normal-state curves one can estimate the contribution in tunneling spectra

from the SC condensate. This work deals with the questions raised above. Tunneling measurements presented in this paper have been performed on overdoped Bi2212 single crystals below and above T_c by break-junctions and in-plane point-contacts, which reveal that the anomaly found in the tunneling $I(V)$ characteristics originates from the SC condensate. In the extracted $I(V)$ characteristics of the SC condensate, the constant asymptotics points to the presence of one-dimensionality in Bi2212. The anomaly found here puts additional constraints on the final theory of SC in the cuprates.

It is important noting that the anomaly in tunneling $I(V)$ curves was already discussed in Ref. [6]; however, in Ref. [6], the anomaly was inferred from abnormally-looking tunneling characteristics. In this work, we show that this anomaly is intrinsically present in any $I(V)$ curve obtained below T_c in Bi2212. Also, the $I(V)$ characteristics measured above T_c were not considered in Ref. [6].

The overdoped Bi2212 single crystals were grown using the self-flux method as described elsewhere [7]. The T_c value was determined by the four-contact method. The transition width is less than 1 K. Experimental details of the measurement setup can be found elsewhere [7]. In short, many break-junctions were prepared by gluing a sample with epoxy on a flexible insulating substrate, and then were broken in the ab -plane by bending the substrate with a differential screw at low temperature in a He ambient. The electrical contacts (typically with the resistance of a few ohms) are made by attaching gold wires to a crystal with silver paint. The $I(V)$ and $dI(V)/dV$ characteristics are determined by the four-terminal method by using the standard lock-in modulation technique. In in-plane SIN tunneling junctions, Pt-Ir wires sharpened mechanically were used as normal tips.

Fig.2a shows SIS tunneling spectra obtained by a break-junction at $T = 8.5$ K in an overdoped Bi2212 single crystal with critical temperature $T_c = 88$ K. The conductance $dI(V)/dV$ exhibits typical features of SIS-junction conductance data in Bi2212: well-defined quasiparticle peaks, a zero-bias peak due to the Josephson current, dips and humps outside the gap structure. As the main result, the $I(V)$ characteristic in Fig.2a is similar to the $I(V)$ curve shown in Fig.1b. The gap magnitude Δ , however, is smaller in the overdoped region. Figure 2b shows a set of tunneling $I(V)$ characteristics obtained in different overdoped Bi2212 single crystals with $T_c = 87 - 89$ K. Comparing Figs.1b, 2a and 2b it is evident that the anomaly is present not only in the underdoped region of Bi2212, but in the overdoped region as well.

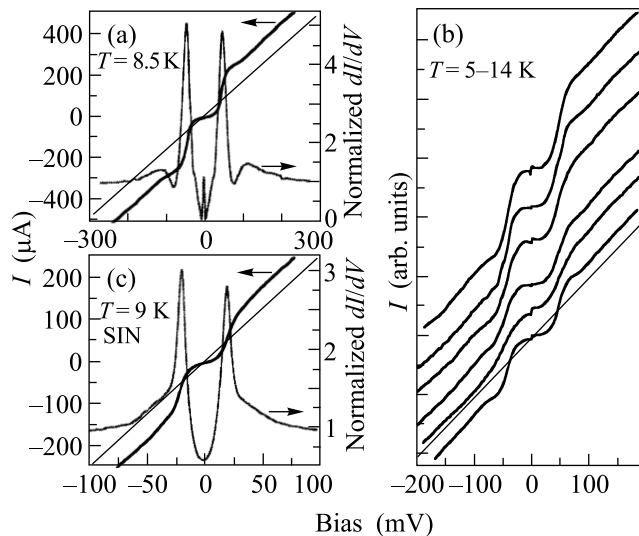


Fig.2. (a) Tunneling $I(V)$ and $dI(V)/dV$ characteristics obtained at $T = 8.5$ K in a SIS junction of an overdoped Bi2212 single crystal with $T_c = 88$ K. (b) Set of $I(V)$ curves obtained at $T = 5 - 14$ K in different overdoped Bi2212 single crystals with $T_c = 87 - 89$ K. The curves are offset for clarity. (c) $I(V)$ and $dI(V)/dV$ characteristics obtained at $T = 9$ K in a SIN junction of an overdoped Bi2212 single crystal with $T_c = 87.5$ K. In all plots, the lines are parallel to the $I(V)$ curves at high bias. The label of the horizontal axis in plot (a) is the same as in plot (c)

Fig.2c depicts tunneling spectra which are similar to those in Fig.2a, but obtained in a SIN junction. Because of the SIN junction, the quasiparticle peaks in the conductance shown in Fig.2c appear at a bias twice smaller than the peak bias in Fig.2a. The $I(V)$ curve in Fig.2c clearly indicates that the observed anomaly is not a SIS-junction effect but an intrinsic feature of tunneling $I(V)$ characteristics obtained in Bi2212.

The next question which we discuss is how to obtain tunneling $I(V)$ characteristics in the normal state. There are, at least, three different solutions. The first two consist in applying a magnetic field below T_c , while the third solution is to measure $I(V)$ above T_c . In the first case, a magnetic field with a magnitude larger than the upper critical magnetic field H_{c2} in Bi2212 renders the whole sample normal. In the second case, by applying a magnetic field with a magnitude larger than the lower critical field H_{c1} , vortices will enter the sample. In the latter case, the normal-state characteristics can be obtained inside vortex cores. Because H_{c2} in Bi2212 is very large, the first solution cannot be realized in laboratory conditions. The second solution seems to be suitable; however, tunneling spectra obtained inside vortex cores have subgap structures which are usually inter-

preted as a manifestation of bound states [8]. Moreover, technically, it is not easy to realize such measurements. So, we are left with the straightforward solution: to measure $I(V)$ characteristics somewhat above T_c . The main disadvantage of measurements performed above T_c is the presence of substantial thermal fluctuations.

Fig.3a depicts tunneling spectra obtained at $T = 119$ K in the same Bi2212 single crystal as those in Fig.2a. Fig.3b presents a set of $I(V)$ curves measured at $T = 115 - 125$ K in different overdoped Bi2212 single crystals. The data in Figs.3a and 3b are obtained in SIS junctions. Fig.3c shows tunneling data obtained in a SIN junction at $T = 117$ K in the same Bi2212 single crystal as those in Fig.2c. The temperatures between 115 and 125 K presented in Fig.3 were not chosen by accident: in slightly overdoped Bi2212, the onset of SC occurs at

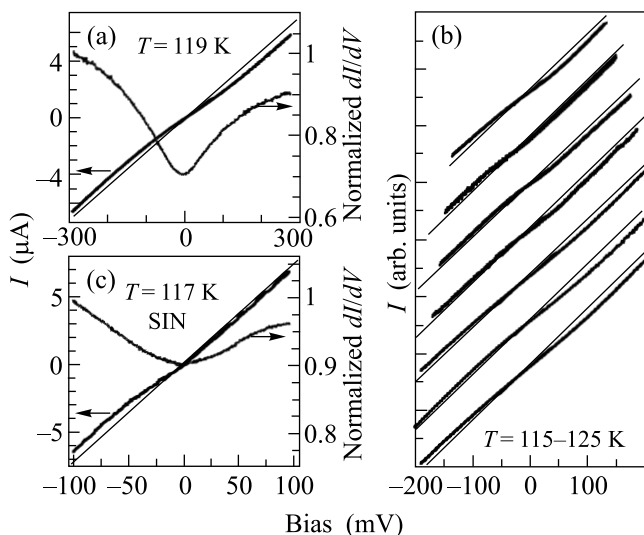


Fig.3. (a) $I(V)$ and $dI(V)/dV$ characteristics obtained at $T = 119$ K in the same SIS junction as those in Fig.2a. (b) Set of $I(V)$ curves obtained at $T = 115 - 125$ K in different overdoped Bi2212 single crystals with $T_c = 87 - 89$ K. The curves are offset for clarity. (c) $I(V)$ and $dI(V)/dV$ characteristics obtained at $T = 117$ K in the same SIN junction as those in Fig.2c. In all plots, the lines are parallel to the $I(V)$ curves at high bias. The label of the horizontal axis in plot (a) is the same as in plot (c)

110–116 K [7]. This temperature range is above the onset of SC in our Bi2212 samples and, as a consequence, the data in Figs.3a–3c mainly provide the contribution from the normal-state pseudogap.

Considering the $I(V)$ characteristics shown in Fig.3, one can see that, at high positive (low negative) bias, they pass somewhat below (above) the line which is parallel to the $I(V)$ curves at high bias. Thus, the anomaly in the $I(V)$ characteristics, found below T_c , vanishes

somewhat above T_c . Then, it is obvious that the anomaly in the $I(V)$ curves originates from the SC condensate. In Fig.3, one can see that the straight line can be used as a first approximation for a normal-state $I(V)$ curve, for example, in Fig.1b. In the $I(V)$ curves measured above T_c , a small “negative” offset from straight lines is caused by the pseudogap: measurements performed in underdoped Bi2212 show that this offset is larger than that in Fig.3. Thus, it scales with magnitude of the pseudogap.

We turn now to the last question raised above. From the tunneling characteristics obtained deep below T_c and somewhat above T_c , by taking the difference between the spectra one can estimate a contribution in the tunneling spectra from the SC condensate. This is equivalent to the procedure usually used in neutron scattering measurements. In our case, however, this procedure only leads to an estimation of the contribution because by subtracting the spectra we assume that the pseudogap crosses T_c without modification. This is not obvious, particularly, at low bias [9].

In order to compare two sets of tunneling spectra, they have to be normalized. The conductance curves can be easily normalized at high bias. How to normalize the corresponding $I(V)$ curves is not a trivial question. The conductance curves at high bias, thus, far away from the gap structure, are almost constant. Consequently, in a SIS junction, by normalizing two conductance curves at high bias, the equation $(dI(V)/dV)_{1,\text{norm}} \simeq (dI(V)/dV)_{2,\text{norm}}$ holds at bias $|V| \gg 2\Delta/e$, where e is the electron charge. By integrating the equation we have $I(V)_{1,\text{norm}} \simeq I(V)_{2,\text{norm}} + C$, where C is the constant, meaning that the corresponding $I(V)_{i,\text{norm}}$ curves are parallel to each other at high bias.

In Fig.4a, the two $I(V)$ characteristics from Figs. 2a and 3a were normalized as described in the previous paragraph: the normal-state $I(V)$ curve is normalized by its value at maximum positive bias, and the $I(V)$ curve from Fig.2a is adjusted to be parallel at high bias to the normalized normal-state curve. Figure 4b depicts their difference as well as the difference between their normalized conductances. The same procedure has been done for the tunneling spectra obtained in a SIN junction, which are shown in Figs. 2c and 3c. The differences are depicted in Fig.4d. The conductances in Figs. 4b and 4d are presented as examples; however, they are not the primary focus of the study: we discuss exclusively the $I(V)$ characteristics. The $I(V)$ data shown in Fig.1b, which are obtained in an underdoped Bi2212 single crystal, went through the same normalization procedure, and the result is presented in Fig.4c. In the latter case, the straight line shown in Fig.1b was used as

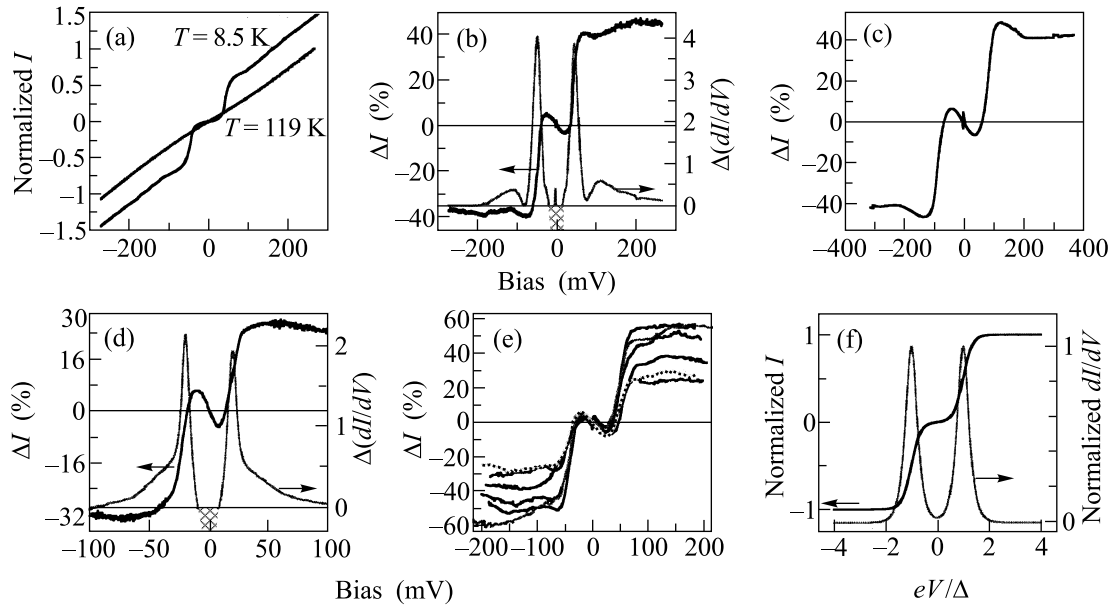


Fig. 4. (a) Two normalized $I(V)$ characteristics from Figs. 2a and 3a, obtained in the same $\text{Bi}2212$ single crystal ($T_c = 88$ K) at different temperatures. The normalization procedure: the normal-state curve is normalized by its value at maximum positive bias, and the other curve is adjusted to be parallel at high bias to the normalized normal-state curve. (b) Difference between the two $I(V)$ curves presented in plot (a), and the difference between their normalized conductances shown in Figs. 2a and 3a. (c) Difference between the $I(V)$ curve and the line, shown in Fig. 1b, which were normalized before subtraction as those in plot (a). The straight line is used as an estimate of the normal-state curve. (d) Difference between the two $I(V)$ curves from Figs. 2c and 3c, normalized before subtraction as those in plot (a), and the difference between their normalized conductances. The data are obtained in a SIN junction. (e) Differences between $I(V)$ characteristics shown in Fig. 2b and their corresponding normal-state curves, normalized before subtraction as those in plot (a). (f) Idealized $I(V)$ characteristic of SC condensate in a SIN junction, and its first derivative. The curves are normalized by their maximum values. In plots (b) and (d), the grey boxes cover the parts of the conductances, which are below zero and have no physical meaning. In plots (b)–(e), the current difference is presented in %. In plots (a) and (b), the labels of horizontal axes are the same as those in plots (c) and (d)

a normal-state curve. The $I(V)$ characteristics shown in Fig. 2b and their corresponding normal-state curves were normalized in the same manner, and the obtained differences are presented in Fig. 4e.

Analyzing the $I(V)$ characteristics shown in Figs. 4b–e, which, in first approximation, represent the contribution from the SC condensate, it is easy to observe the general trends of the curves. First, at high bias, the curves reach a plateau value. Second, at the gap bias, the curves rise/fall sharply. Last, at low bias, the curves go to zero. In Figs. 4b–e, the negative slope of the curves at low bias, implying a negative differential resistance, is an artifact. This artifact is simply a consequence of the rough estimation used here [9]. *Tout ensemble*, Figure 4f depicts an idealized $I(V)$ characteristic summarizing the observed tendencies. The first derivative of the $I(V)$ characteristic is also shown in Fig. 4f. The constant asymptotics of the $I(V)$ characteristic are the fingerprints of the presence of one-dimensionality in the system [6]. In Figs. 4b–e, one can see that the contribution from the SC condensate in these $I(V)$ characteristics at high bias is 25–55 % above

the contribution from the pseudogap. It is *important* noting that the asymptotics of some $I(V)$ curves obtained in $\text{Bi}2212$ below T_c look similar to those in Fig. 1a; however, the anomaly discussed here always appears in the difference obtained between two normalized $I(V)$ curves measured *below* and *above* T_c in one sample.

As shown elsewhere [6], the $I(V)$ characteristic in Fig. 4f can be fitted by the hyperbolic function $f(V) = A \times (\tanh[(eV - \Delta)/eV_0] + \tanh[(eV + \Delta)/eV_0])$, where e is the electron charge; V is the bias; Δ is the maximum SC gap, and A and V_0 are the constants. The conductance $dI(V)/dV$ curve can be well fitted by the derivative $[f(V)]' = A_1 \times (\text{sech}^2[(eV - \Delta)/eV_0] + \text{sech}^2[(eV + \Delta)/eV_0])$. The hyperbolic \tanh and sech^2 fits are in good agreement with predictions of the bisoliton model [10] which is based on the nonlinear Schrödinger equation. The bisoliton theory utilizes the concept of bisolitons—electron (or hole) pairs coupled in a singlet state due to local deformation of the lattice [10].

Finally, it is worth mentioning that the anomaly found here is also present in an $I(V)$ characteristic obtained in optimally doped $\text{YBa}_2\text{C}_3\text{O}_{6.95}$ [11].

It is interesting that the anomaly is also present in the $I(V)$ characteristics measured in some *non*-superconducting materials—in the stripe-ordered perovskite $\text{La}_{1.4}\text{Sr}_{1.6}\text{Mn}_2\text{O}_7$ [12] and in quasi-one-dimensional charge-density-wave conductor NbSe_3 [13] (in NbSe_3 , the anomaly is at zero bias). However, this issue is already beyond the scope of this study, and will be discussed elsewhere.

In summary, tunneling measurements have been carried out on slightly overdoped $\text{Bi}_2\text{Sr}_2\text{CaCu}_2\text{O}_{8+x}$ single crystals below and above T_c by break-junctions and point-contacts. An anomaly was found in the tunneling $I(V)$ characteristics. Analysis of the data shows that the anomaly is caused by the superconducting condensate. The constant asymptotics of the $I(V)$ characteristic of the condensate, shown in Fig.4f, are the fingerprints of the presence of one-dimensionality in $\text{Bi}2212$ [6]. The anomaly found here puts additional constraints on the final theory of high- T_c superconductivity.

I would like to thank N. Miyakawa for sending the data from Ref.[5], Yu. I. Latyshev for sending unpublished data related to Ref.[13], and V. Z. Kresin for comments on the manuscript.

1. J. G. Bednorz and K. A. Müller, *Z. Phys.* **B64**, 189 (1986).
2. J. Orenstein and A. J. Millis, *Science* **288**, 468 (2000).
3. A. V. Fedorov, T. Valla, P. D. Johnson et al., *Phys. Rev. Lett.* **82**, 2179 (1999).
4. G. E. Blonder, M. Tinkham, and T. M. Klapwijk, *Phys. Rev.* **B25**, 4515 (1982).
5. N. Miyakawa, P. Guptasarma, J. F. Zasadzinski et al., *Phys. Rev. Lett.* **80**, 157 (1998).
6. A. Mourachkine, *Europhys. Lett.* **55**, 559 (2001).
7. A. Mourachkine, *Europhys. Lett.* **49**, 86 (2000).
8. S. H. Pan, E. W. Hudson, A. K. Gupta et al., *Phys. Rev. Lett.* **85**, 1536 (2000).
9. Crossing T_c from above, the pseudogap undergoes a strong renormalization of quasiparticle excitations at low bias (see Fig.3 in Ref. [3]).
10. A. S. Davydov, *Phys. Rep.* **190**, 191 (1990).
11. A. G. Sun, A. Truscott, A. S. Katz et al., *Phys. Rev.* **B54**, 6734 (1996).
12. T. Nachtrab, S. Heim, M. Mössle et al., *Phys. Rev.* **B65**, 012410 (2002).
13. Yu. I. Latyshev, A. A. Sinchenko, L. N. Bulaevskii et al., *JETP Lett.* **75**, 103 (2002).